CEP receptor signalling controls root system architecture in Arabidopsis and Medicago

Kelly Chapman[1], Ariel Ivanovici[1], Michael Taleski[1], Craig Sturrock[2], Jason L. P. Ng[1], Nadiatul A. Mohd-Radzman[1], Florian Frugier[3], Malcolm Bennett[4], Ulrike Mathesius[1] and Michael A. Djordjevic[1,*]

[1] Division of Plant Sciences, Research School of Biology, The Australian National University, Canberra, ACT 2601, Australia

[2]The Hounsfield Facility, University of Nottingham, Sutton Bonington Campus, Loughborough. LE12 5RD, UK

[3] Institute of Plant Sciences Paris-Saclay (IPS2), CNRS, Univ Paris Sud, Univ Paris Diderot, INRA, Univ d'Evry, Université Paris-Saclay, 91190 Gif-sur-Yvette, France

[4]School of Biosciences, University of Nottingham, Sutton Bonington Campus, Loughborough LE12 5RD, UK

[*] Corresponding author (telephone +61 2 61253088; email: michael.djordjevic@anu.edu.au)

Total word count: 4679 words

Summary: 192 words

Introduction: 1148 words

Methods and Materials: 1410 words

Results: 1265 words

Discussion: 856 words

Acknowledgements: 198 words

No. figures: 9

No. Supporting information: 4 figures, 2 videos

Summary

- Root system architecture (RSA) influences the effectiveness of resources acquisition from soils but the genetic networks that control RSA remain largely unclear.
- We used rhizoboxes, X-ray Computed Tomography, grafting, auxin transport measurements and hormone quantification to demonstrate that Arabidopsis and Medicago CEP (C-TERMINALLY ENCODED PEPTIDE)-CEP RECEPTOR signalling controls RSA, the gravitropic set-point angle (GSA) of lateral roots (LRs), auxin levels, and auxin transport.
- We showed that soil-grown Arabidopsis and Medicago CEP receptor mutants have a narrower RSA, which results from a steeper LR GSA. Grafting shows that CEPR1 in the shoot controls GSA. CEP receptor mutants exhibited an increase in rootward auxin transport and elevated shoot auxin levels. Consistently, the application of auxin to wild-type shoots induced a steeper GSA and auxin transport inhibitors counteracted the CEP receptor mutant's steep GSA phenotype. Concordantly, CEP peptides increased GSA and inhibited rootward auxin transport in WT but not in CEP receptor mutants.
- The results indicate that CEP-CEP receptor-dependent signalling outputs in Arabidopsis and Medicago control overall RSA, LR GSA, shoot auxin levels and rootward auxin transport. We propose that manipulating CEP signalling strength or CEP receptor downstream targets may provide means to alter RSA.

Keywords

CEP, CEPR1, CRA2, gravitropic set-point angle, lateral root, peptide hormone, rootward auxin transport, root system architecture.

Introduction

Plant roots acquire vital resources from soils to support growth, productivity and survival. The spatial configuration of the root system in soil, termed root system architecture (RSA), results from an interplay between hard-wired and plastic developmental programs. Their developmental plasticity enables roots to alter their intrinsic growth patterns in response to diverse soil signals (Rellán-Álvarez *et al.*, 2015) and this ability is thought to have allowed vascular plants to more effectively colonise diverse terrestrial ecosystems throughout evolution. For example, these adaptive responses enable root systems to forage for important heterogeneously-dispersed resources such as water, phosphorous, potassium and nitrate (Giehl & von Wirén, 2014; Morris *et al.*, 2017; Orosa-Puente *et al.*, 2018; Jia *et al.*, 2019).

Lateral roots (LRs) are major determinants of RSA. LR initiation in Arabidopsis involves the division of specific pericycle cells (Casimiro *et al.*, 2001; Dubrovsky *et al.*, 2008; Moreno-Risueno *et al.*, 2010). By contrast, pericycle, endodermal and cortical cells participate in LR initiation in many other plants such as *Medicago truncutula* (named Medicago hereafter) (Herrbach *et al.*, 2014). Although many studies focus on LR initiation (Lavenus *et al.*, 2013; Porco *et al.*, 2016), it is the growth, density, and the subsequent trajectory of LRs through soil that collectively determine RSA (Rellán-Álvarez *et al.*, 2015; Chapman *et al.*, 2019). The gene networks and complex developmental outputs that control RSA and their adaptive responses to external stimuli, however, remain poorly understood.

Auxin plays critical roles in the growth and development of LRs including their positioning, initiation, outgrowth, and emergence (reviewed in Du and Scheres (2017); Banda *et al.* (2019)). Auxin itself and alteration of genes that control auxin level and sensitivity also influence the angle at which LRs grow away from the main root of agar plate-grown plants (Rosquete *et al.*, 2013; Roychoudhry *et al.*, 2013). This angle of LR growth relative to the gravity vector is termed the gravitropic set point angle (GSA) (Wang *et al.*, 2015). After initiating in the main root at a 90° angle from the gravity vector, LRs tilt down shortly after emerging with a specific initial GSA, which is defined at stage III of LR emergence (Rosquete *et al.*, 2013; Rosquete *et al.*, 2018). This initial GSA influences RSA by ensuring that LRs explore the soil at distance from the main root. Genes that affect auxin transport, sensitivity, perception and synthesis e.g. *PIN2*, *PIN3*, *PIN4*, *PIN7*, *AUX1*, *TIR1*, *WEI8*, *TAR2*, *YUC1*, *AXR3*, *NPH4*, *AFR19* and *EXOCYST70A3* play positive or negative roles in LR GSA and root depth (Rosquete *et al.*, 2013; Roychoudhry & Kepinski, 2015; Wang *et al.*, 2017;

Giri *et al.*, 2018; Ogura *et al.*, 2019). Additional changes to the GSA occur as the LRs grow away from the main root and this may enable the further reorientation of their growth towards the gravity vector, thus imparting an even more-steeply angled RSA (Rellán-Álvarez *et al.*, 2015). There is, however, little understanding of the regulatory networks that link auxin to LR GSA, and it is unknown if auxin in the rootward transport stream and/or local auxin synthesis or sensitivity controls GSA. Recently, the modulation of the root GSA by an actin binding protein, RMD (Huang *et al.*, 2018), and auxin transport by *EXOCYST70A3* were found to play roles in shaping root system depth (Ogura *et al.*, 2019).

In Arabidopsis, C-TERMINALLY ENCODED PEPTIDEs (CEPs) and CEP RECEPTOR1 play a role in controlling root organogenesis and, in particular, LR growth and development (Imin *et al.*, 2013; Tabata *et al.*, 2014; Mohd-Radzman *et al.*, 2015; Mohd-Radzman *et al.*, 2016; Roberts *et al.*, 2016; Taleski *et al.*, 2016; Taleski *et al.*, 2018; Chapman *et al.*, 2019). For example, Chapman *et al.* (2019) showed using grafting studies that local and systemic CEP-CEPR1 signalling negatively controls LR growth in response to shoot-derived sucrose by affecting LR meristem size and length of mature root cells. Consistently, Tabata *et al.* (2014) noted that the *cepr1-1* mutant has increased LR growth but the underlying mechanism was not explored. Tabata *et al.* (2014) and Ohkubo *et al.* (2017) defined a role for CEP peptides in long distance nitrogen-demand signalling responses that result in the control of the expression of nitrate transporters in the roots of plants grown under heterogeneous nitrate levels. It is not known if this nitrogen-demand signalling response is related to the alteration of root growth in *cepr1-1*.

In Medicago, the interaction of the MtCEP1 peptide with the putative CEPR1 orthologue, named COMPACT ROOT ARCHITECTURE 2 (CRA2), decreases the number of LRs per plant (Imin *et al.*, 2013; Huault *et al.*, 2014; Mohd-Radzman *et al.*, 2016; Laffont *et al.*, 2019). This negative effect of MtCEP1 on LR formation counteracts an auxin-dependent stimulation of LR number (Mohd-Radzman *et al.*, 2015). Although CEP peptide signalling affects root development across monocot and dicot species (Ohyama *et al.*, 2008; Delay *et al.*, 2013; Imin *et al.*, 2013; Mohd-Radzman *et al.*, 2015; Mohd-Radzman *et al.*, 2016; Sui *et al.*, 2016), they affect main root and lateral root growth to different extents. For example, CEP peptide addition results in the inhibition of main root growth in Arabidopsis, but not in Medicago (Delay *et al.*, 2013; Imin *et al.*, 2013). Therefore, it is important to identify conserved CEP-CEPR1 signalling mechanisms across species. In addition, whilst CEP-CEPR1/CRA2 signalling differentially controls the extent of LR growth in Arabidopsis and

Medicago in agar plate-grown plants, it is not known whether CEPs can influence GSA or RSA when grown in soil.

There is increasing interest in developing crops with steeply-angled RSAs because they are better adapted at intercepting mobile soil resources such as nitrate and water (Lynch, 2013; Lynch & Wojciechowski, 2015). Therefore, identifying conserved genes and mechanisms across plant species that control the formation of steeply-angled RSAs is important for crop breeding initiatives aiming to improve the efficiency of resource acquisition (Singh et al., 2011; Voss-Fels et al., 2018). The lack of readily-available systems to visualise RSA in soil in laboratory settings, however, hampers the progress of fundamental research in this area.

This study focuses on determining if CEP-CEPR1 signalling controls RSA in agar plate and soil grown plants. To explore how Arabidopsis roots grow in soil, we used a simple rhizobox system to enable the progressive visualisation of RSA over time. This rhizobox system circumvented the limitations of current X-ray CT approaches to detect the thin roots of Arabidopsis and examine overall RSA. Using our rhizobox system and X-ray CT, respectively, we then demonstrated that Arabidopsis and Medicago CEP receptor mutants share steeply-angled RSAs in soil compared to wild-type (WT) plants. Grafting studies then showed that shoot-located CEP receptors controlled LR GSA in both species. The overall results suggested that CEPs interact with CEP receptors to affect the auxin pool size and rootward auxin transport. The identification of congruent effects of CEP hormone signalling across species enabled us to propose a model where CEP-CEPR1/CRA2 controls GSA most likely by affecting shoot auxin pools and/or rootward auxin transport.

Materials and Methods

Plant materials and growth conditions

In *Arabidopsis thaliana*, the No-0 *cepr1-1* (RATM11-2459; RIKEN) (Bryan *et al.*, 2012; Tabata *et al.*, 2014) and Col-0 *cepr1-3* (467C01; GABI-Kat) (Kleinboelting *et al.*, 2012; Chapman *et al.*, 2019) mutants were used. Sterilised Arabidopsis seeds were grown on solidified media (1% Type M agar) containing ½ strength Murashige–Skoog (MS) basal salts (Sigma) at pH 5.7 and 1% w/v sucrose. In *Medicago truncatula*, the A17 *cra2-11* and *cra2-13* (previously named *tr185*) (Bourion *et al.*, 2014; Huault *et al.*, 2014; Laffont *et al.*, 2019) and R108 *cra2-1* mutants were used. Medicago seeds were prepared as described in Imin *et al.* (2013), and grown on solidified Fåhraeus medium (Holmes *et al.*, 2008) containing 5 mM KNO_3. Plates were grown in chambers at 22 °C with 100-120 µmol m^{-2} s^{-1} light and a 16 h

photoperiod. Roots were scanned on a flatbed scanner at 600 dpi and root angles measured using ImageJ. GSA was measured as the angle between 1.5mm from the point of LR emergence and the gravity vector, for LRs with a straight plateau phase (Rosquete *et al.*, 2013; Rosquete *et al.*, 2018)

Auxin application to shoots

For shoot treatments, a 1 mM stock of 1-Naphthaleneacetic acid (NAA; Sigma) dissolved in DMSO was diluted to 1 µM in water. A 10 µL droplet was added to the leaves or between the cotyledons of Arabidopsis and Medicago plants, respectively, and the solution was replenished each day.

Auxin transport inhibitor treatments

A 10 mM stock of 2,3,5-Triiodobenzoic acid (TIBA), and a 1 mM stock of *N*-1-naphthylphthalamic acid (NPA) (Sigma) were dissolved in DMSO and added to the autoclaved medium to the final concentrations described.

Synthetic CEP peptide treatments

Synthetic AtCEP3 (TFRhyPTEPGHShyPGIGH; > 95% purity; hyP represents hydroxyl-Proline) and MtCEP1 (AFQhyPTTPGNShyPGVGH, at >95% purity) peptides were dissolved in water and used at 1 µM (Delay *et al.*, 2013; Imin *et al.*, 2013; Mohd-Radzman *et al.*, 2015). Peptides were synthesised by GL Biochem, Shanghai and their structures validated independently by mass spectrometry. Peptides were added to the medium as previously described (Delay *et al.*, 2013; Imin *et al.*, 2013).

Rhizobox system for viewing Arabidopsis root system architecture

Seedlings were grown in pots with soil for 3 weeks prior to being transferred to rhizoboxes. Rhizoboxes adapted for the growth of Arabidopsis (Whiting *et al.*, 2000) were made from 100 mm square petri dishes with a slot cut into the lid. Rhizoboxes were completely filled with a compacted seed raising mix (Debco, Bella Vista NSW). Seedlings were transferred to rhizoboxes, and at the time of transfer, the main root of pot-grown seedlings was ~ 30 mm long and lacked visibly-emerged LRs. Therefore, most of the growth of the root system occurred post-transfer to the rhizoboxes. Water (3 mL) was added to the soil to prevent the roots from drying out. The slot cut into the lid was placed over the hypocotyl of the seedling such that the shoot was exterior to the rhizobox. The rhizobox lids were secured with

masking tape. Rhizoboxes were placed in a tray with a clear cover to maintain humidity and minimise evaporation. Rhizoboxes were placed at a 60° angle with the lid on the underside to encourage root growth on the soil-plate interface, and scanned weekly. The architecture of the root system was analysed using the GLORIA plugin for ImageJ (Rellán-Álvarez *et al.*, 2015).

X-ray Computed Tomography (CT) analysis of Medicago RSA in soil

A17 WT or *cra2-11* were grown in sieved (<2 mm) sandy loam soil uniformly packed to a bulk density of 1.1 mg/m^3 in a 68 mm (diameter) x 160 mm (height) cylindrical column made from high density poly ethylene (Mairhofer *et al.*, 2017) for 21 days in a Conviron A1000 growth chamber at 22 ˚C, 60% humidity with a 16 hour photoperiod. After 14- and 21-days growth, each column was scanned using a GE v|tome|x M 240 kV X-ray CT system at the Hounsfield Facility, University of Nottingham. Scans were made in 'fast mode', collecting a single radiograph image for each of the 2400 angular projections over a 360˚ rotation of the sample at spatial resolution of 40 µm. Scans were made in 3 sections to obtain the full length of the column/soil depth. Data were reconstructed and subjected to manual root segmentation techniques to digitally separate the roots from the soil. Extracted root system architectures were quantified using ROOTH software (Mairhofer *et al.*, 2017) for total root length, branch structure and LR angle.

Hypocotyl grafting

Arabidopsis seedlings were grown for 6 days on ½ MS with 0.5% sucrose prior to hypocotyl grafting (Branco & Masle, 2019). Five days after grafting, plants were transferred to ½ MS medium with 1% sucrose. For Medicago grafting, the cotyledons were removed from five-day-old seedlings prior to cutting the hypocotyl. A vertical incision (~5mm) was made in the hypocotyl of the rootstock to create a junction. The scion was inserted into the vertically-cut tissue and root systems were scored after five weeks.

Auxin Quantification by UPLC-MS/MS

Roots and shoots from six-day old A17 and *cra2-11* mutant were separated, snap frozen, and stored at ˉ80 ˚ C until required. Frozen tissue samples were ground using 4 mm stainless steel beads (Bearing shop online, Queensland) in a Qiagen TissueLyser LT with a precooled tube holder. To each tube 20 µL of the internal standard (1 µg/mL of 3-[$^2H_5$] indolylacetic acid) followed by 1 mL extraction solvent (20% methanol:79% propanol:1% glacial acetic acid)

were added and auxin extraction was performed in a sonicator bath for 15 min at 4°C. The extraction and analytical procedures for auxins were adapted from Ng *et al.* (2015), with modifications to the analytical procedure as follows.

The UPLC-MS/MS procedure was performed using the Thermo QE Plus UPLC-Orbitrap with the following parameters. Samples and standards were injected (5 µL) onto an Agilent Zorbax Eclipse 1.8 µm XDB-C18 2.1 × 50 mm column. Solvent A consisted of 0.1% aqueous formic acid and solvent B consisted of 90% methanol/water with 0.1% formic acid. Free auxins and conjugates were eluted with a linear gradient from 10 to 50% solvent B over 8 min, 50 to 70% solvent B from 8 to 12 min (then held at 70% from 12 to 20 min) at a flow rate of 200 µL min^{-1}. The eluted samples were introduced into the mass spectrometer via a heated electrospray ionisation (HESI-II) probe and analysed with the Q-Exactive Plus Orbitrap (Thermo Scientific, Waltham, MA, USA). The HESI was operated in the positive mode with the following parameters: ultra-high purity nitrogen gas was used as the sheath gas (45 L min^{-1}), auxiliary gas (10 L min^{-1}) and sweep gas (2 L min^{-1}); the spray voltage was 3.5 kV; capillary temperature was 250 ^{o}C; the S-lens RF level was 50 V; the auxiliary gas heater temperature was 300 ^{o}C. Tandem mass spectrometry was carried out using the parallel reaction monitoring mode with a mass resolution of 17,500 at 1.0 microscan. The Automatic Gain Control target value was set at 1.0E+05 counts, maximum accumulation time was 50 ms and the isolation window was set at m/z 4.0. Data were acquired and analysed using the Thermo Scientific Xcalibur 4.0 software.

Auxin transport measurements

For auxin transport measurements, a tritium-labelled IAA (^{3}H-IAA; 22 mCi/mmol; Vitrax Placentia, CA, USA) solution was prepared in ethanol (van Noorden *et al.*, 2006) and 2 µL applied to the shoot apical meristem of six-day old Medicago or Arabidopsis seedlings. In Medicago A17 WT and *cra2-11* mutants, the seedlings were treated with 1 µM MtCEP1 or a water control for 48 hours prior to ^{3}H-IAA application. Plants were grown for a further four hours after ^{3}H-IAA application before roots were harvested. In Medicago, roots were harvested below the hypocotyl junction in four 4 mm segments, whereas in Arabidopsis roots were harvested in two 10 mm segments. For auxin transport measurements in decapitated roots, ^{3}H-IAA was mixed with 1% agarose and cut into 2x2x2 mm blocks that were applied to excised R108 WT and *cra2-1* roots as described in Ng *et al.* (2015). Where indicated, 1 µM TIBA was added to roots 24 hours prior to ^{3}H-IAA application. For all auxin transport

analyses, root segments were placed in 200 µL of Microscint-40: water mixture (3:1) in OptiPlate-96 microplates (Perkin Elmer). Microplates were sealed with TopSeal-A Plus, incubated overnight in the dark, and shaken vigorously for 10 s on a plate shaker (Perkin Elmer). The radioactivity of samples was analysed in a MicroBeta2 Microplate Counter (Perkin Elmer).

Results

CEPR1 controls root system width in soil-grown Arabidopsis

Visualising Arabidopsis RSA in soil is challenging due to their narrow, fragile root system. To address this, we developed a cheap and effective method to observe Arabidopsis RSA in soil using a simple, modified rhizobox system (Whiting *et al.*, 2000). We observed that *cepr1-1* and *cepr1-3* mutants displayed a narrower root system compared to their respective WT lines (Fig **1a-c**). This difference in RSA became apparent after one to two weeks of rhizobox growth (Fig. **1b,c**; Fig. **S1a,b**). For example, two-weeks after transfer of seedlings from pots to rhizoboxes, the root system widths of *cepr1-1* and *cepr1-3* were ~26% and ~52% of their WTs, respectively. The narrower root system phenotype of the *cepr1* mutants persisted over the four week growth period (Fig. **1b,c**; Fig. **S1**). WT plants displayed wider root systems with a more even distribution of LRs in the soil (Fig. **1b,c**; Fig. **S1**) in contrast to the *cepr1* mutants which displayed root systems with a comparatively high density (Fig. **1a**; Fig. **S1)**. Therefore, *CEPR1* loss of function in two Arabidopsis ecotypes results in a major and comparable perturbation of RSA, which can be observed readily using our rhizobox setup.

CRA2 signalling controls RSA in soil-grown Medicago

To determine if CEP-CEP receptor signalling is conserved across species, we imaged the RSA phenotype of Medicago WT (A17) and *cra2-11* grown in soil using X-ray CT at 14 and 21 days post-germination (Fig. **2a,b**; Video **S1**; Video **S2**). The LRs of WT emerged at an angle of ~84˚ and there was no significant alteration to this initial trajectory as the LRs grew away from the main root towards the container's wall (Fig. **2a,b**; Video **S1**). Contact with the container's wall caused the WT LRs to grow downwards, as clearly seen in the day 21 images (Fig. **2a,b**). By contrast, *cra2* LRs emerged at a reduced angle of ~73˚ and, contrary to WT LRs, their growth trajectory progressively aligned towards the gravity vector by day 21 (Fig. **2a,b**; Video **S2**). This resulted in the *cra2* LRs failing to reach the container's side wall, thus imparting a steeper angled RSA.

CEPR1/CRA2 signalling controls LR GSA

Based on the decreased root system width of the *CEP* receptor mutants (Fig. **1a-c)**, we hypothesised that CEP-CEPR1 signalling affected Arabidopsis LR GSA. To test this, we measured the LR GSA of Arabidopsis WT and *cepr1* seedlings grown on agar plates with, or without, exogenous CEP peptide addition (Fig. **3 a,b,** Fig. **S2a**). Consistent with the narrower root system of rhizobox-grown *cepr1* mutants, the LRs of *cepr1-1* and *cepr1-3* mutants grew with an 11-12 ° reduction in GSA relative to their respective WTs (Fig. **3 a,b**). Concordantly, the treatment of WT plants with AtCEP3 peptides increased GSA by 7-15 °, whereas *cepr1-1* and *cepr1-3* mutants were insensitive to AtCEP3 (Fig. **3 a.b;** Fig. **S2a**), as expected for CEP receptor knockout mutants. These results indicate that CEP-CEPR1 signalling affects root system width by increasing LR GSA, consistent with CEP peptide addition inducing the opposite phenotypic effect of a *CEPR1* knockout.

To test if the effect of CEP addition on GSA was conserved in Medicago, we examined agar plate-grown A17 WT and *cra2-11* mutants in the presence or absence of MtCEP1 peptides. Consistently, the *cra2-11* mutant had a ~13 ° decrease in the LR GSA compared to the A17 WT, and the MtCEP1 treatment increased the LR GSA by ~18 ° in the WT, but not in *cra2-11* (Fig. **3c,** Fig. **S2b**). These results reveal that the CEP-CEPR1/CRA2 pathway affects LR GSA similarly in Fabaceae and Brassicaceae.

CEPR1/CRA2 control LR GSA from the shoot via auxin

Prior publications reported that CEPR1 controls local (root) and systemic (shoot) LR growth in Arabidopsis whereas CRA2 controls LR number locally in Medicago (Huault *et al.*, 2014; Roberts *et al.*, 2016; Tabata *et al.*, 2014; Mohd-Radzman *et al.*, 2015; Chapman *et al.*, 2019; Delay *et al.*, 2019; Laffont *et al.*, 2019). Therefore, we grafted hypocotyls of Arabidopsis WT and *cepr1* mutants and Medicago A17 and *cra2-11* to determine if the CEP receptor controls the GSA from the root and/or the shoot (Fig. **4a-c**). The results clearly demonstrate that *CEPR1/CRA2* controls LR GSA from the shoot in both species.

Given that *CEPR1/CRA2* controls LR GSA from the shoot and that both auxin and auxin transport play a fundamental role in controlling LR GSA (Rosquete *et al.*, 2013; Roychoudhry *et al.*, 2013), we assessed if shoot-applied auxin influences root GSA in agar plate grown plants. The application of NAA droplets (10 µL per day, 10^{-6} M) to Arabidopsis or Medicago shoots over several days resulted in a reduction of LR GSA in WT (Fig. **5a-d**). This reduction in GSA mimicked the reduced LR GSA of CEP receptor mutants. However,

NAA failed to further alter the GSA of CEP receptor mutants, suggesting no further shoot auxin-dependent reduction in GSA was possible in *cepr1* or *cra2* mutants. These results show that an increase in shoot auxin levels phenocopies the GSA phenotype of CEP receptor mutants.

CEP receptor mutants have higher shoot IAA, IAA-Ala, and rootward auxin transport

Next, we determined if auxin levels were altered in Medicago A17 WT and *cra2-11* mutant roots and/or shoots by quantitatively assessing the levels of several auxin derivatives using mass spectrometry (Fig. **6**; Fig. **S3**). The results revealed IAA and IAA-Ala levels were significantly increased in *cra2-11* shoots (Fig. **6**), whereas other auxin species showed no significant difference (Fig. **S3**). There was also no significant difference in auxin species content between WT and *cra2-11* roots (Fig. **6**; Fig. **S3**).

We hypothesised that an increase in shoot auxin may lead to an alteration in rootward auxin transport (Bhalerao *et al.*, 2002). To assess this, we determined the effect of MtCEP1 in A17 WT and *cra2-11* mutants on polar auxin transport. To do so, we measured radiolabelled IAA accumulation in root segments following the precise application of radiolabelled IAA to the shoot apex. MtCEP1 reduced the quantum of radiolabelled IAA in several consecutive root segments in the A17 WT, but not in *cra2-11* (Fig. **7a**), indicating that the MtCEP1-mediated reduction of shoot-to-root auxin transport depends on the CRA2 CEP receptor. Moreover, there was an increased basal auxin transport level in *cra2-11* compared to the A17 WT control. The increase in auxin transport observed in consecutive roots segments of the A17 *cra2-11* mutant was also recapitulated in the *cra2-1* mutant in the R108 genotype (Fig. **7b**), again indicating a conservation of CEP-CEP receptor signalling.

We next measured auxin transport in both Arabidopsis *cepr1* mutants and their respective WTs. Consistent with Medicago *cra2* mutants either in A17 or R108 genotypes, we detected an increase in auxin transport in both *cepr1* mutants (Fig. **7c,d**). Together, these results suggest that CEP-CEP receptor signalling reduces auxin transport across diverse plant species.

Auxin transport inhibitors counteract the steeper GSA of CEP receptor mutants.

Auxin transport inhibitors are known to increase GSA (Rosquete *et al.*, 2013). If a decreased GSA in *cepr1* mutants is attributable to increased auxin transport, we would expect auxin transport inhibitors to counteract this phenotype. In Medicago, the addition of TIBA to roots

abolished auxin transport in R108 WT and *cra2-1* mutants (Fig. **8a)**. In addition, we found that root applied TIBA increased the GSA of Arabidopsis and Medicago CEP receptor mutants (Fig. **8b-d,** Fig. **S4a,b)** and another independent auxin transport inhibitor, NPA, similarly increases *cepr1-1*'s GSA (Fig. **8e**). Collectively, these results suggest that the CEP-CEP receptor signalling may affect GSA by reducing rootward auxin transport and/or by altering auxin levels in shoots, and that this response is conserved between Fabaceae and Brassicaceae plants.

Discussion

RSA is a trait of agronomic importance as it influences the effective interception and capture of soil resources and thus plant productivity and survival (Morris *et al.*, 2017; Pandey & Bennett, 2019). This complex trait is controlled by the interaction of multiple developmental processes, hence different regulatory pathways are likely to regulate multiple RSA features depending on environmental cues. In this study, we showed that we could image Arabidopsis and Medicago roots using a simple rhizobox system or X-ray CT, respectively, to show that CEP-CEP receptor signalling plays a major and conserved role in shaping RSA across these Fabaceae and Brassicaceae species by affecting the trajectory of LR growth in soil. This is notable since some other CEP-CEP receptor mediated processes that control root growth (e.g. main root growth, LR growth and density), are not entirely congruent between Medicago and Arabidopsis (Delay *et al.*, 2013; Imin *et al.*, 2013; Huault *et al*., 2014; Tabata *et al.*, 2014; Djordjevic *et al.*, 2015; Mohd-Radzman *et al.*, 2015; Mohd-Radzman *et al.*, 2016; Roberts *et al.*, 2016; Chapman *et al.*, 2019; Delay *et al.*, 2019; Laffont *et al.*, 2019).

Medicago and Arabidopsis CEP receptor mutants share a shoot-controlled steeply angled RSA and an increase in rootward auxin transport. Increased levels of shoot auxin were also demonstrated for Medicago CEP receptor mutants. In addition, the discrete application of small droplets of NAA to shoot tissues to WT in both species phenocopies the steeply angled RSA of their respective CEP receptor mutants. From these findings, we conclude that a likely role of CEP-CEP receptor signalling is to modulate RSA as a consequence of decreasing auxin levels in shoots and/or by reducing rootward auxin transport as presented in the model in Fig. **9**. Whilst the increased levels of IAA and IAA-Ala in Medicago *cra2* shoots are consistent with this conclusion, further work would be needed to determine if auxin concentration in the shoot alone, increased auxin transport to the root, or both, is/are causal for the steeper GSA in CEP-receptor mutants. Nevertheless, these data are consistent with a

large body of work which implicates auxin perception, transport, level or sensitivity in controlling LR GSA (Rosquete *et al.*, 2013; Roychoudhry *et al.*, 2013) and root depth (Ogura *et al.*, 2019). We cannot, however, discount the involvement of other mobile rootward signals that are influenced by CEP-CEPR1 signalling (Tabata *et al*., 2014; Ohkubo *et al*., 2017).

Prior studies have revealed that CEP-CEP receptor signalling pathways play multiple roles in controlling main root and LR growth in Arabidopsis and LR and nodule number in Medicago (Delay *et al.*, 2013; Imin *et al.*, 2013; Huault *et al.*, 2014; Tabata *et al.*, 2014; Djordjevic *et al.*, 2015; Mohd-Radzman *et al.*, 2015; Mohd-Radzman *et al.*, 2016; Shabala *et al.*, 2016; Taleski *et al.*, 2016; Taleski *et al.*, 2018; Chapman *et al.*, 2019; Delay *et al.*, 2019; Laffont *et al.*, 2019) in addition to the roles we describe here in RSA and GSA. There is evidence that some CEP-CEP receptor signalling responses are controlled by distinct mechanisms; for example CEP-dependent lateral root density is controlled by local root responses in Medicago (Huault *et al*., 2014; Laffont et al., 2019), in contrast to the shoot controlled root responses described here. Hence, CEP-CEP receptor signalling appears to impact various aspects of root development via local and systemic pathways which together impart a major influence on root system developmental plasticity across species.

Root GSA is known to change in response to levels of soil nutrients to aid their foraging (Lynch, 2018). For example, Huang *et al.* (2018) demonstrated recently that low phosphate soils caused GSA to become shallower by increasing expression of the actin binding protein RMD, which interfered with the root gravity perception machinery. In contrast, *CEP* gene transcription is modulated by nitrate and carbon levels (Delay *et al.*, 2013; Imin *et al.*, 2013; Tabata *et al.*, 2014; Chapman *et al.*, 2019), abiotic stress (Delay *et al.*, 2013), and biotic signals (Imin *et al.*, 2013). Hence, we propose that the strength of activation of local and systemic CEP-CEP receptor signalling is likely to play a role in integrating the adaptive response of roots to fluctuating environments. This is consistent with CEP-CEP receptor signalling controlling the extent of the use of shoot-derived carbon to drive root system growth (Chapman *et al.*, 2019).

Since *CEP* genes evolved in seed plants (Angiosperms and Gymnosperms) (Ogilvie *et al.*, 2014), and *CEP* and *CEPR1* gene expression is localised in root and shoot vascular tissues (Imin *et al.*, 2013; Roberts *et al.*, 2013; Tabata *et al.*, 2014; Roberts *et al.*, 2016), we speculate that the CEP-CEP receptor signalling pathway evolved to enable vascular plants to adapt to diverse environments limited in resources by providing a mechanism to modulate

root growth and architecture as well as the trajectory of LR growth through soils. Moreover, CEP-CEP receptor signalling may have evolved to modulate pre-existing auxin-mediated signalling mechanisms present in earlier plant lineages. Therefore, the diversity of CEP peptides, the strength of CEP affinity for CEP receptors, the persistence of CEP signalling, and downstream effectors of CEP receptors provide a variety of targets for molecular breeders aiming to manipulate crop RSA.

Acknowledgements

This work was supported by an Australian Research Council grant to MAD (DP150104250); AI was supported by an A.W. Howard fellowship and Nicolas Baudin travel award, and FF was supported by Centre National de la Recherche Scientifique, the Agence Nationale de la Recherche Labex "Saclay Plant Science" and Lidex "Plant Phenotyping Pipeline"; MT, AI and KC were supported by an Australian Post Graduate awards. Financial support by the Access to Research Infrastructures activity in the Horizon 2020 Programme of the EU (EPPN2020 Grant Agreement 731013-) is gratefully acknowledged. NAMR's current address is the Sainsbury Laboratory, University of Cambridge, Cambridge. Discussions with Dr Nijat Imin, University of Auckland, are graciously acknowledged.

Author contributions

MAD, MT, AI, MB and KC devised experiments and wrote the manuscript. FF provided genetic material and participated in drafting the manuscript. NMR contributed preliminary data on CEP effects on LR growth trajectory. JN, UM, AI, and KC did the auxin transport measurements and auxin quantification assays using mass spectrometry resources at the ANU's Joint Mass Spectrometry Facility, Canberra, Australia. KC and AI obtained data for all other figures and MT and MAD devised Fig. 9. MAD and CJS did the quantification of Medicago RSA using X-ray CT.

References

Banda J, Bellande K, von Wangenheim D, Goh T, Guyomarc'h S, Laplaze L, Bennett MJ. 2019. Lateral Root Formation in Arabidopsis: A Well-Ordered LRexit. *Trends in Plant Science* **24**(9): 826-839.

Bhalerao RP, Eklöf J, Ljung K, Marchant A, Bennett M, Sandberg G. 2002. Shoot-derived auxin is essential for early lateral root emergence in Arabidopsis seedlings. *The Plant Journal* **29**(3): 325-332.

Bourion V, Martin C, de Larambergue H, Jacquin F, Aubert G, Martin-Magniette M-L, Balzergue S, Lescure G, Citerne S, Lepetit M, et al. 2014. Unexpectedly low nitrogen acquisition and absence of root architecture adaptation to nitrate supply in a Medicago truncatula highly branched root mutant. *Journal of Experimental Botany* **65**(9): 2365-2380.

Branco R, Masle J. 2019. Systemic signalling through translationally controlled tumour protein controls lateral root formation in Arabidopsis. *Journal of Experimental Botany* **70**(15): 3927-3940.

Bryan A, Obaidi A, Wierzba M, Tax F. 2012. XYLEM INTERMIXED WITH PHLOEM1, a leucine-rich repeat receptor-like kinase required for stem growth and vascular development in Arabidopsis thaliana. *Planta* **235**(1): 111-122.

Casimiro I, Marchant A, Bhalerao RP, Beeckman T, Dhooge S, Swarup R, Graham N, Inzé D, Sandberg G, Casero PJ, et al. 2001. Auxin Transport Promotes Arabidopsis Lateral Root Initiation. *The Plant Cell* **13**(4): 843-852.

Chapman K, Taleski M, Ogilvie HA, Imin N, Djordjevic MA. 2019. CEP–CEPR1 signalling inhibits the sucrose-dependent enhancement of lateral root growth. *Journal of Experimental Botany* **70**(15): 3955-3967.

Delay C, Chapman K, Taleski M, Wang Y, Tyagi S, Xiong Y, Imin N, Djordjevic MA. 2019. CEP3 levels affect starvation-related growth responses of the primary root. *Journal of Experimental Botany* **70**(18): 4763-4774.

Delay C, Imin N, Djordjevic MA. 2013. CEP genes regulate root and shoot development in response to environmental cues and are specific to seed plants. *Journal of Experimental Botany* **64**(17): 5383-5394.

Djordjevic MA, Mohd-Radzman NA, Imin N. 2015. Small-peptide signals that control root nodule number, development, and symbiosis. *Journal of Experimental Botany* **66**(17): 5171-5181.

Du Y, Scheres B. 2017. Lateral root formation and the multiple roles of auxin. *Journal of Experimental Botany* **69**(2): 155-167.

Dubrovsky JG, Sauer M, Napsucialy-Mendivil S, Ivanchenko MG, Friml J, Shishkova S, Celenza J, Benková E. 2008. Auxin acts as a local morphogenetic trigger to specify lateral root founder cells. *Proceedings of the National Academy of Sciences* **105**(25): 8790-8794.

Giehl RFH, von Wirén N. 2014. Root Nutrient Foraging. *Plant Physiology* **166**(2): 509-517.

Giri J, Bhosale R, Huang G, Pandey BK, Parker H, Zappala S, Yang J, Dievart A, Bureau C, Ljung K, et al. 2018. Rice auxin influx carrier OsAUX1 facilitates root hair elongation in response to low external phosphate. *Nature Communications* **9**(1): 1408.

Herrbach V, Remblière C, Gough C, Bensmihen S. 2014. Lateral root formation and patterning in Medicago truncatula. *Journal of Plant Physiology* **171**(3): 301-310.

Holmes P, Goffard N, Weiller GF, Rolfe BG, Imin N. 2008. Transcriptional profiling of Medicago truncatulameristematic root cells. *BMC Plant Biology* **8**(1): 21.

Huang G, Liang W, Sturrock CJ, Pandey BK, Giri J, Mairhofer S, Wang D, Muller L, Tan H, York LM, et al. 2018. Rice actin binding protein RMD controls crown root angle in response to external phosphate. *Nature Communications* **9**(1): 2346.

Huault E, Laffont C, Wen J, Mysore KS, Ratet P, Duc G, Frugier F. 2014. Local and Systemic Regulation of Plant Root System Architecture and Symbiotic Nodulation by a Receptor-Like Kinase. *PLOS Genetics* **10**(12): e1004891.

Imin N, Mohd-Radzman NA, Ogilvie HA, Djordjevic MA. 2013. The peptide-encoding CEP1 gene modulates lateral root and nodule numbers in Medicago truncatula. *Journal of Experimental Botany* **64**(17): 5395-5409.

Jia Z, Giehl RFH, Meyer RC, Altmann T, von Wirén N. 2019. Natural variation of BSK3 tunes brassinosteroid signaling to regulate root foraging under low nitrogen. *Nature Communications* **10**(1): 2378.

Kleinboelting N, Huep G, Kloetgen A, Viehoever P, Weisshaar B. 2012. GABI-Kat SimpleSearch: new features of the Arabidopsis thaliana T-DNA mutant database. *Nucleic Acids Research* **40**(D1): D1211-D1215.

Laffont C, Huault E, Gautrat P, Endre G, Kalo P, Bourion V, Duc G, Frugier F. 2019. Independent Regulation of Symbiotic Nodulation by the SUNN Negative and CRA2 Positive Systemic Pathways. *Plant Physiology*: pp.01588.02018.

Lavenus J, Goh T, Roberts I, Guyomarc'h S, Lucas M, De Smet I, Fukaki H, Beeckman T, Bennett M, Laplaze L. 2013. Lateral root development in Arabidopsis: fifty shades of auxin. *Trends in Plant Science* **18**(8): 450-458.

Lynch JP. 2013. Steep, cheap and deep: an ideotype to optimize water and N acquisition by maize root systems. *Annals of Botany* **112**(2): 347-357.

Lynch JP, Wojciechowski T. 2015. Opportunities and challenges in the subsoil: pathways to deeper rooted crops. *Journal of Experimental Botany* **66**(8): 2199-2210.

Lynch JP. 2018. Rightsizing root phenotypes for drought resistance. *Journal of Experimental Botany* **69**(13): 3279-3292.

Mairhofer S, Pridmore T, Johnson J, Wells DM, Bennett MJ, Mooney SJ, Sturrock CJ. 2017. X-Ray Computed Tomography of Crop Plant Root Systems Grown in Soil. *Current Protocols in Plant Biology* **2**(4): 270-286.

Mohd-Radzman NA, Binos S, Truong TT, Imin N, Mariani M, Djordjevic MA. 2015. Novel MtCEP1 peptides produced in vivo differentially regulate root development in Medicago truncatula. *Journal of Experimental Botany* **66** (17): 5289-5300.

Mohd-Radzman NA, Laffont C, Ivanovici A, Patel N, Reid DE, Stougaard J, Frugier F, Imin N, Djordjevic MA. 2016. Different pathways act downstream of the peptide receptor CRA2 to regulate lateral root and nodule development. *Plant Physiology*.

Moreno-Risueno MA, Van Norman JM, Moreno A, Zhang J, Ahnert SE, Benfey PN. 2010. Oscillating Gene Expression Determines Competence for Periodic Arabidopsis Root Branching. *Science* **329**(5997): 1306-1311.

Morris EC, Griffiths M, Golebiowska A, Mairhofer S, Burr-Hersey J, Goh T, von Wangenheim D, Atkinson B, Sturrock CJ, Lynch JP, et al. 2017. Shaping 3D Root System Architecture. *Current Biology* **27**(17): R919-R930.

Ng JLP, Hassan S, Truong TT, Hocart CH, Laffont C, Frugier F, Mathesius U. 2015. Flavonoids and Auxin Transport Inhibitors Rescue Symbiotic Nodulation in the Medicago truncatula Cytokinin Perception Mutant cre1. *The Plant Cell* **27**(8): 2210-2226.

Ohyama K, Ogawa M, Matsubayashi Y. 2008. Identification of a biologically active, small, secreted peptide in Arabidopsis by in silico gene screening, followed by LC-MS-based structure analysis. *The Plant Journal* **55**(1): 152-160.

Ogilvie HA, Imin N, Djordjevic MA. 2014. Diversification of the C-TERMINALLY ENCODED PEPTIDE (CEP) gene family in angiosperms, and evolution of plant-family specific CEP genes. *BMC Genomics* **15**(1): 870.

Ogura T, Goeschl C, Filiault D, Mirea M, Slovak R, Wolhrab B, Satbhai SB, Busch W. 2019. Root System Depth in Arabidopsis Is Shaped by EXOCYST70A3 via the Dynamic Modulation of Auxin Transport. *Cell* **178**(2): 400-412.e416.

Ohkubo Y, Tanaka M, Tabata R, Ogawa-Ohnishi M, Matsubayashi Y. 2017. Shoot-to-root mobile polypeptides involved in systemic regulation of nitrogen acquisition. *Nature Plants* **3**: 17029.

Orosa-Puente B, Leftley N, von Wangenheim D, Banda J, Srivastava AK, Hill K, Truskina J, Bhosale R, Morris E, Srivastava M, et al. 2018. Root branching toward water involves posttranslational modification of transcription factor ARF7. *Science* **362**(6421): 1407-1410.

Pandey BK, Bennett MJ. 2019. A New Angle on How Roots Acclimate to Sporadic Rainfall. *Cell* **178**(2): 269-271.

Porco S, Larrieu A, Du Y, Gaudinier A, Goh T, Swarup K, Swarup R, Kuempers B, Bishopp A, Lavenus J, et al. 2016. Lateral root emergence in Arabidopsis is dependent on transcription factor LBD29 regulation of auxin influx carrier LAX3. *Development* **143**(18): 3340-3349.

Rellán-Álvarez R, Lobet G, Lindner H, Pradier P-L, Sebastian J, Yee M-C, Geng Y, Trontin C, LaRue T, Schrager-Lavelle A. 2015. GLO-Roots: an imaging platform enabling multidimensional characterization of soil-grown root systems. *Elife* **4**: e07597.

Roberts I, Smith S, Rybel BD, Van Den Broeke J, Smet W, De Cokere S, Mispelaere M, De Smet I, Beeckman T. 2013. The CEP family in land plants: Evolutionary analyses, expression studies, and role in Arabidopsis shoot development. *Journal of Experimental Botany* **64**(17): 5371-5381.

Roberts I, Smith S, Stes E, De Rybel B, Staes A, van de Cotte B, Njo MF, Dedeyne L, Demol H, Lavenus J, et al. 2016. CEP5 and XIP1/CEPR1 regulate lateral root initiation in Arabidopsis. *Journal of Experimental Botany* **67**(16): 4889-4899.

Rosquete MR, von Wangenheim D, Marhavý P, Barbez E, Stelzer Ernst HK, Benková E, Maizel A, Kleine-Vehn J. 2013. An auxin transport mechanism restricts positive orthogravitropism in lateral roots. *Current Biology* **23**(9): 817-822.

Rosquete MR, Waidmann S, Kleine-Vehn J. 2018. PIN7 Auxin Carrier Has a Preferential Role in Terminating Radial Root Expansion in Arabidopsis thaliana. *International Journal of Molecular Sciences* **19**(4): 1238.

Roychoudhry S, Del Bianco M, Kieffer M, Kepinski S. 2013. Auxin Controls Gravitropic Setpoint Angle in Higher Plant Lateral Branches. *Current Biology* **23**(15): 1497-1504.

Roychoudhry S, Kepinski S. 2015. Shoot and root branch growth angle control — the wonderfulness of lateralness. *Current Opinion in Plant Biology* **23**: 124-131.

Shabala S, White RG, Djordjevic MA, Ruan Y-L, Mathesius U. 2016. Root-to-shoot signalling: integration of diverse molecules, pathways and functions. *Functional Plant Biology* **43**(2): 87-104.

Singh V, van Oosterom EJ, Jordan DR, Hunt CH, Hammer GL. 2011. Genetic Variability and Control of Nodal Root Angle in Sorghum. *Crop Science* **51**(5): 2011-2020.

Sui Z, Wang T, Li H, Zhang M, Li Y, Xu R, Xing G, Ni Z, Xin M. 2016. Overexpression of Peptide-Encoding OsCEP6.1 Results in Pleiotropic Effects on Growth in Rice (O. sativa). *Frontiers in Plant Science* **7**(228).

Tabata R, Sumida K, Yoshii T, Ohyama K, Shinohara H, Matsubayashi Y. 2014. Perception of root-derived peptides by shoot LRR-RKs mediates systemic N-demand signaling. *Science* **346**(6207): 343-346.

Taleski M, Imin N, Djordjevic MA. 2016. New role for a CEP peptide and its receptor: complex control of lateral roots. *Journal of Experimental Botany* **67**(16): 4797-4799.

Taleski M, Imin N, Djordjevic MA. 2018. CEP peptide hormones: key players in orchestrating nitrogen-demand signalling, root nodulation, and lateral root development. *Journal of Experimental Botany* **69**(8): 1829-1836.

van Noorden GE, Ross JJ, Reid JB, Rolfe BG, Mathesius U. 2006. Defective Long-Distance Auxin Transport Regulation in the Medicago truncatula super numeric nodules Mutant. *Plant Physiology* **140**(4): 1494-1506.

Voss-Fels KP, Robinson H, Mudge SR, Richard C, Newman S, Wittkop B, Stahl A, Friedt W, Frisch M, Gabur I, et al. 2018. VERNALIZATION1 Modulates Root System Architecture in Wheat and Barley. *Molecular Plant* **11**(1): 226-229.

Wang H-Z, Yang K-Z, Zou J-J, Zhu L-L, Xie ZD, Morita MT, Tasaka M, Friml J, Grotewold E, Beeckman T, et al. 2015. Transcriptional regulation of PIN genes by FOUR LIPS and MYB88 during Arabidopsis root gravitropism. *Nature Communications* **6**: 8822.

Wang L, Guo M, Li Y, Ruan W, Mo X, Wu Z, Sturrock CJ, Yu H, Lu C, Peng J, et al. 2017. LARGE ROOT ANGLE1, encoding OsPIN2, is involved in root system architecture in rice. *Journal of Experimental Botany* **69**(3): 385-397.

Whiting SN, Leake JR, McGrath SP, Baker AJM. 2000. Positive responses to Zn and Cd by roots of the Zn and Cd hyperaccumulator Thlaspi caerulescens. *New Phytologist* **145**(2): 199-210.

Figure legends

Figure 1. CEPR1 signalling controls overall root system architecture and root system width in soil-grown Arabidopsis

WT and *cepr1* mutants in the Col-0 and No-0 ecotypes were grown in rhizoboxes over a four week period. (**a**) Representative images of Arabidopsis WT (left) and *cepr1* mutants (right) in the No-0 (top) and Col-0 (bottom) ecotypes four weeks after transfer to rhizoboxes (Scale bar=10 mm). (**b,c**) Weekly measurements of root system width in No-0 (**b**) and Col-0 (**c**) WT and *cepr1* (n≥4 plants) (Student's t-test; *, P≤0.05; **, P≤0.01; ***, P≤0.001) (error bars, ±SE). Similar results were obtained in three independent experiments.

Figure 2. CRA2 signalling controls RSA in soil-grown Medicago

(**a, b**) X-ray Computed Tomography scan images of Medicago A17 WT and *cra2-11* mutants grown in soil for (**a**) 14 days and (**b**) 21 days. Scale bar=20 mm. (**c**) Root angle relative to the point of emergence at positions along the length of the LR (n=3 plants). Different letters indicate a statistically significant difference (P≤0.05, two-way ANOVA followed by Tukey multiple comparisons test) (error bars, ±SE).

Figure 3. CEP peptide-CEPR1/CRA2 signalling controls the GSA of LRs

(**a-c**) Stage III LR GSA root angle of 12 day old WT and *cepr1* mutants in Arabidopsis and Medicago grown with or without CEP peptides. Arabidopsis plants in the No-0 (**a**) and Col-0 (**b**) genotypes were grown with or without 1µM AtCEP3 peptide on agar plates (n=60 LRs from 10 plants). Medicago **(c)** A17 WT and *cra2-11* mutant plants were grown with or without 1 µM MtCEP1 peptide on agar plates (n≥ 79 LRs from 24 plants). Different letters indicate a statistically significant difference (P≤ 0.05, two-way ANOVA followed by Tukey multiple comparisons test) (error bars, ±SE).

Figure 4. CEPR1/CRA2 controls LR GSA from the shoot

Arabidopsis WT and *cepr1* mutants, or Medicago WT and *cra2* mutants, were reciprocally shoot/root grafted and LR GSA root angle was measured upon recovery of growth. (**a**) Arabidopsis No-0 and *cepr1-1* mutant plants nine days after grafting (n=40 LRs from 8 plants). (**b**) Arabidopsis Col-0 and *cepr1-3* mutant plants ten days after grafting (n=40 LRs

from 6 plants). (**c**) Medicago A17 WT and *cra2-11* mutants five weeks after grafting (n=14-29 LRs from 8 plants). Different letters indicate a statistically significant difference (P≤0.05, two-way ANOVA followed by Tukey multiple comparisons test) (error bars, ±SE).

Figure 5. Shoot application of NAA decreases WT LR GSA.

Arabidopsis plants were grown for 7 days prior to addition of 10 µL of 1 µM NAA or water (control) to the shoot. Solutions were then supplied at 24 hour intervals for 3 days. The GSA was measured when plants were 10 days old: (**a**) WT No-0 and *cepr1-1* (n ≥ 28 LRs from 8 plants) and (**b**) WT Col-0 and *cepr1-3* (n ≥ 15 LRs from 8 plants). (**c**, **d**) Medicago plants were grown for 4 days prior to addition of 10 µL of 1 µM NAA or water (control) to the shoot apical meristem. Solutions were then supplied at 24 hour intervals for 3 days. The GSA was measured when plants were 7 days old: (**c**) WT A17, *cra2-11* and *cra2-13* (n≥ 38 LRs from 18 plants) and (**d**) WT R108 and *cra2-1* (n≥35 LRs from 18 plants). Different letters indicate a statistically significant difference (P≤0.05, two-way ANOVA followed by Tukey multiple comparisons test) (error bars, ±SE).

Figure 6. A CEP receptor knockout leads to higher IAA and IAA-Ala levels in Medicago shoots

Roots and shoots from 6-day old WT A17 and *cra2-11* were extracted and the level of several auxin derivatives was quantitatively assessed using mass spectrometry by spiking in standards into samples. Concentration of (**a**) IAA and (**b**) IAA-Alanine (n=5, pools of 50 roots or 25 shoots) (Student's t-test, **, P≤0.01) (error bars, ±SE).

Figure 7. CEP receptor mutants display increased auxin transport

(**a,b**) Levels of radiolabelled IAA transported in root segments of 7 day old WT and *cra2* mutants in Medicago. The root segment S1 is the closest to the site of application, and higher numbered segments are further away from the site of application of the radiolabelled IAA. (**a**) WT A17 and *cra2-11* mutant seedlings were grown for 6 days and radiolabelled IAA was applied to the shoot apex 4 h prior to harvesting root segments. MtCEP1 1µM was applied to roots 48 h prior to radiolabelled IAA addition (n ≥ 25) (P≤0.05, two-way ANOVA followed by Tukey multiple comparisons test) (error bars, ± SE). (**b**) WT R108 and *cra2-1* mutant seedlings were grown for 6 days and auxin blocks were applied to excised roots 16 mm above

the root tip, with the 4 mm segment in contact with the auxin block discarded (Ng *et al.*, 2015) (n ≥ 30). (**c,d**) Levels of radiolabelled IAA transported in root segments of seven day old WT and *cepr1* mutants in Arabidopsis No-0 (**c**) or Col-0 (**d**) genotypes (n≥17) (Student's t-test,*, P≤0.05; **, P≤0.01; ***, P≤0.001) (error bars, ±SE).

Figure 8. Auxin transport inhibitors counteract the steep GSA phenotype of CEP receptor mutants.

(**a**) WT R108 and *cra2-1* mutant seedlings were grown for 5 days before roots were flood treated with 1µM TIBA for 24 hours. Auxin blocks were applied to excised roots 16 mm above the root tip, with the 4 mm segment in contact with the auxin block discarded. The root segment S1 is the closest to the site of application, and higher numbered segments are further away from the site of application of the radiolabelled IAA (Ng *et al.*, 2015) (n ≥ 25). (**b-e**) LR GSA of WT and CEP receptor mutants grown for 12 days in the presence or absence of auxin transport inhibitors. *Medicago* WT A17 and *cra2-11* mutants (**b**), *Arabidopsis* WT No-0 and *cepr1-1* mutants (**c**), and WT Col-0 and *cepr1-3* mutants (**d**) were grown in the presence or absence of 1µM TIBA (n≥21 LR from ≥8 plants). (**e**) WT No-0 and *cepr1-1* mutants were grown with or without 10 µM NPA (n≥12 LR from 8 plants) (P≤0.05, two-way ANOVA followed by Tukey multiple comparisons test) (error bars, ±SE).

Figure 9. A model for CEP-CEPR1/CRA2 control of the LR GSA.

CEP peptides act through CEPR1/CRA2 to increase (make shallower) the LR GSA. Conversely, Arabidopsis and Medicago CEP receptor mutants have a steep LR GSA phenotype, which is dictated by the loss of CEPR1/CRA2 activity in the shoot. Arabidopsis and Medicago CEP receptor mutants also display elevated shoot auxin levels and/or rootward auxin transport capacity. Moreover, shoot application of auxin to WT plants results in a steeper LR GSA, which phenocopies the CEP receptor GSA. Auxin transport inhibitors counteract the steep LR GSA phenotype of CEP receptor mutants, consistent with shoot-to-root auxin transport affecting LR GSA. Therefore, increased rootward auxin transport in the CEP receptor mutants may lead to increased accumulation of auxin in lateral roots resulting in a steeper LR GSA and ultimately a narrower RSA. It is possible that other rootward signal(s) may also be involved in CEP receptor-dependent control of LR GSA.

Supporting Information

Figure S1. Development of Arabidopsis roots in rhizoboxes at weekly intervals.

Figure S2. Representative images of root GSA measurements in Arabidopsis and Medicago.

Figure S3. Low abundance IAA conjugate levels did not differ between WT A17 and *cra2-11* in Medicago.

Figure S4. LRs treated with TIBA reoriented their GSA with the gravity vector in Arabidopsis.

Video S1. X-ray CT scan of a representative Medicago WT A17 at 14 and 21 days.

Video S2. X-ray CT scan of a representative Medicago *cra2-11* mutant at 14 and 2

Figure 1. CEPR1 signalling controls root system width in soil-grown Arabidopsis.

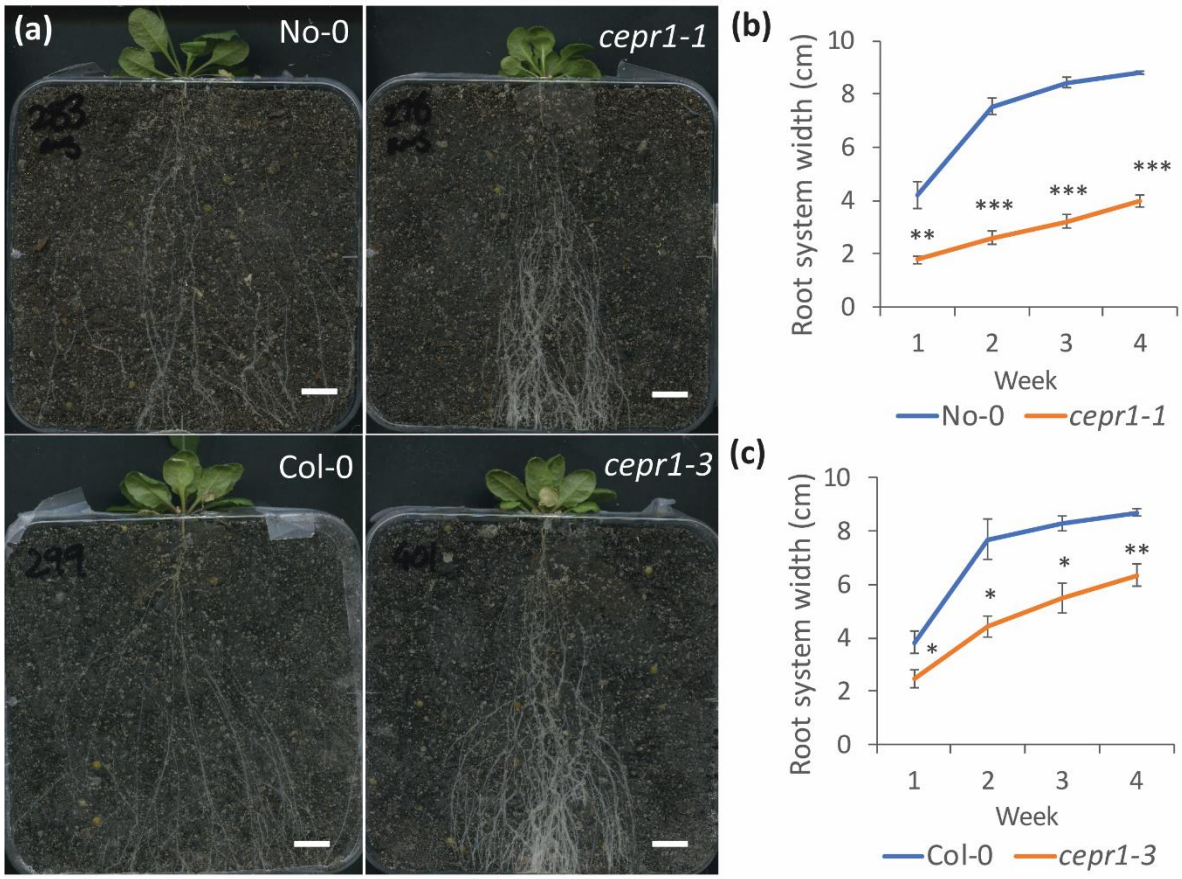

Figure 2. CRA2 signalling controls RSA in soil-grown Medicago.

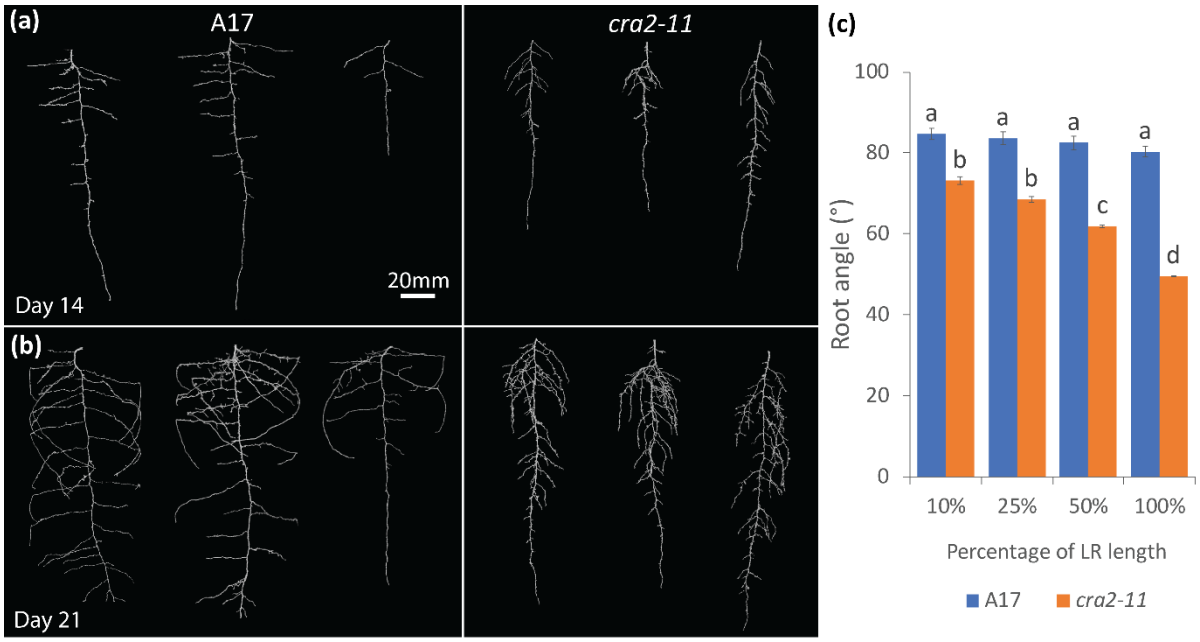

Figure 3. CEP-CEPR signaling affects LR GSA.

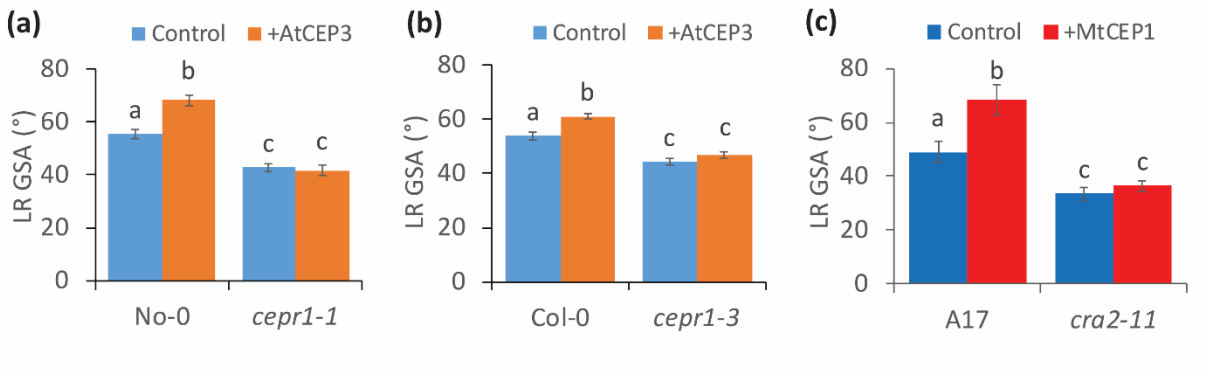

Figure 4. LR GSA is controlled by *CEPR1/CRA2* in the shoot.

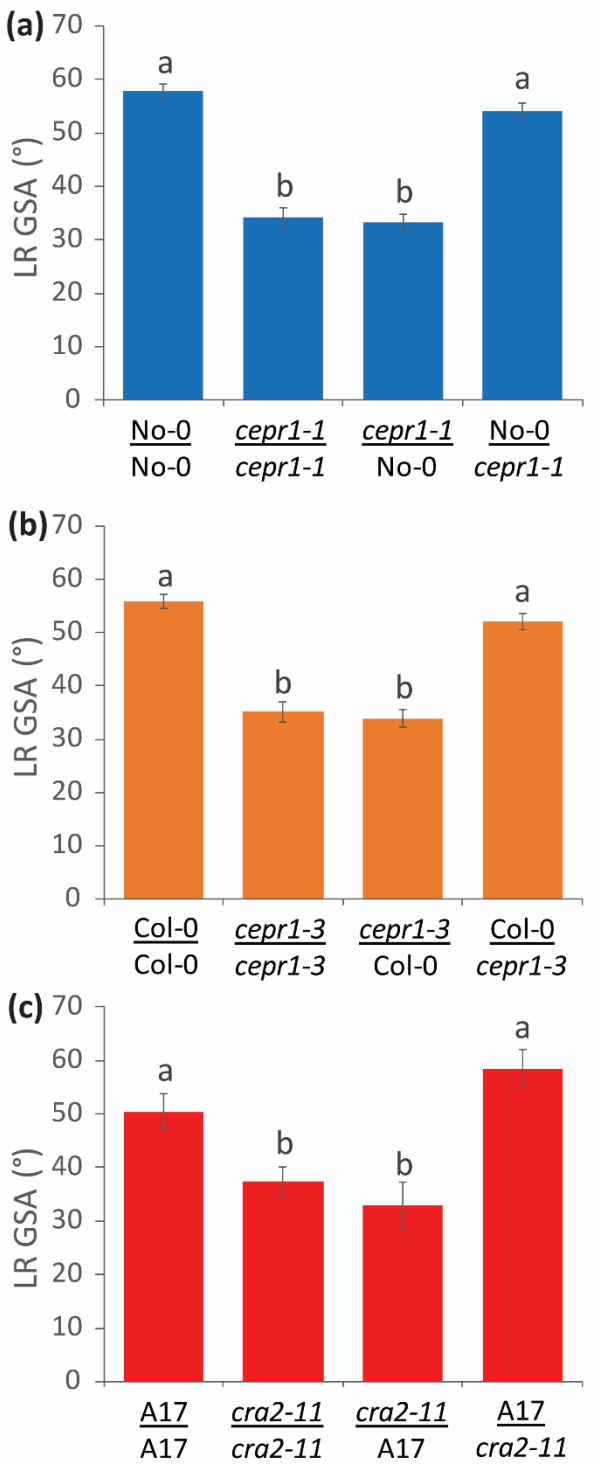

Figure 5. Shoot application of NAA decreases WT LR GSA.

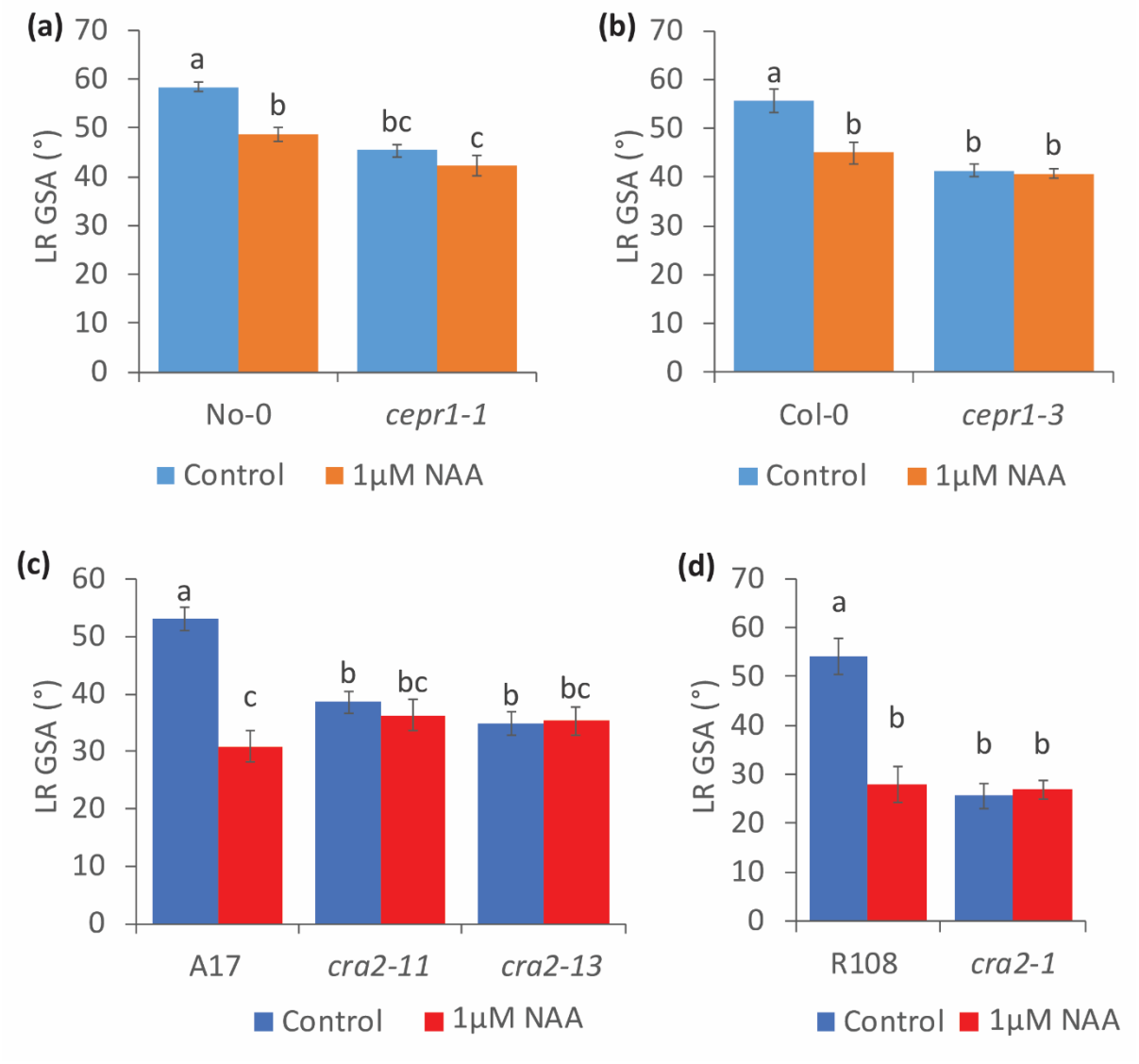

Figure 6. CEP receptor knockout leads to higher IAA and IAA-Ala levels in Medicago shoots.

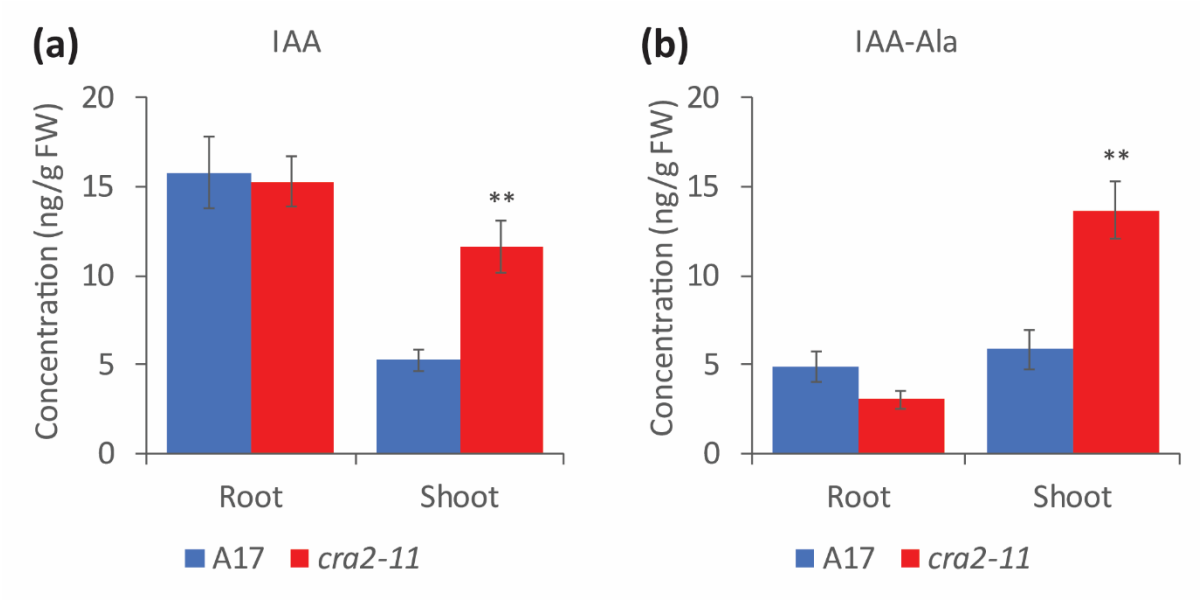

Figure 7. CEP receptor mutants display increased auxin transport.

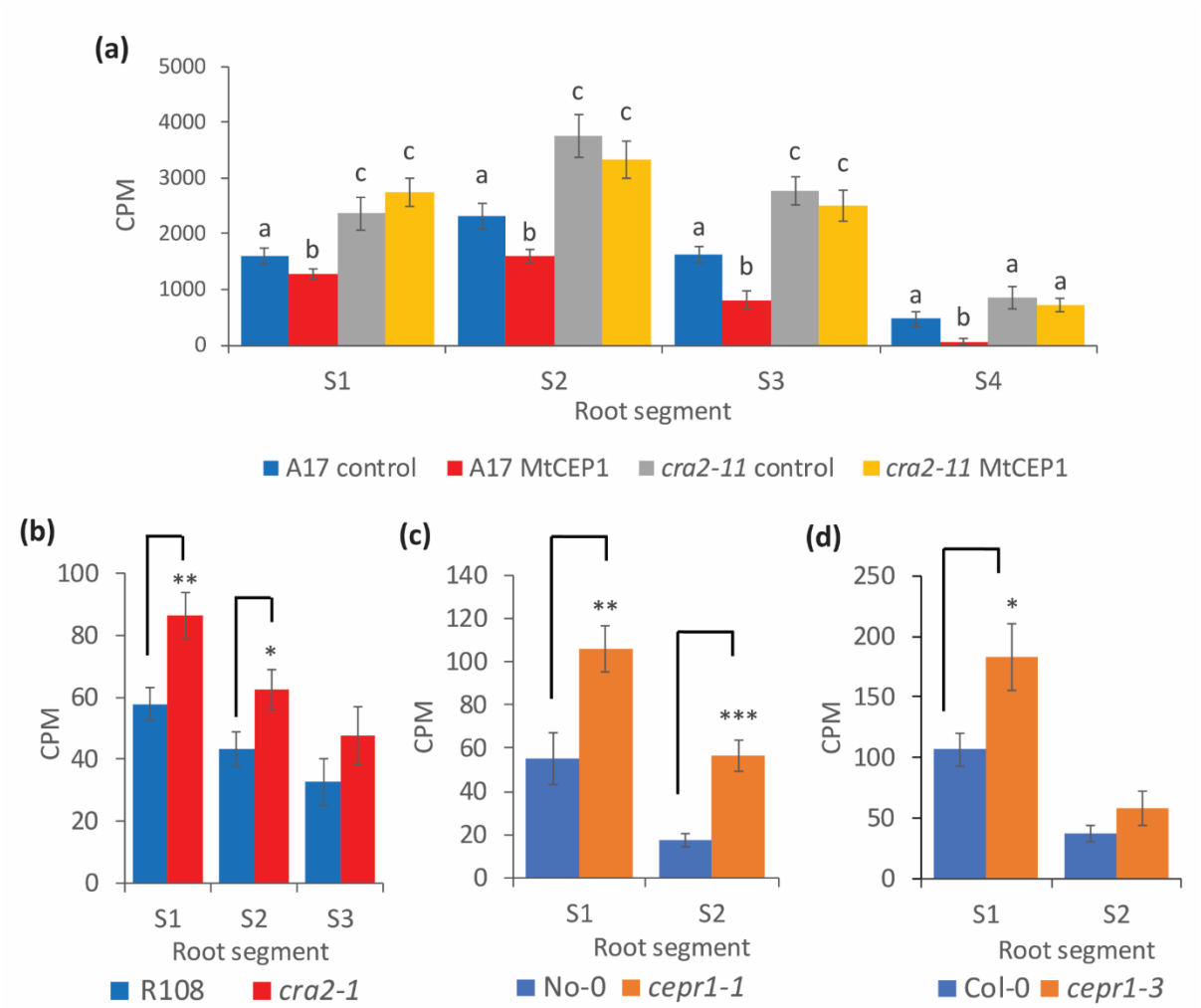

Figure 8. Auxin transport inhibitors counteract the steep GSA phenotype of CEP receptor mutants.

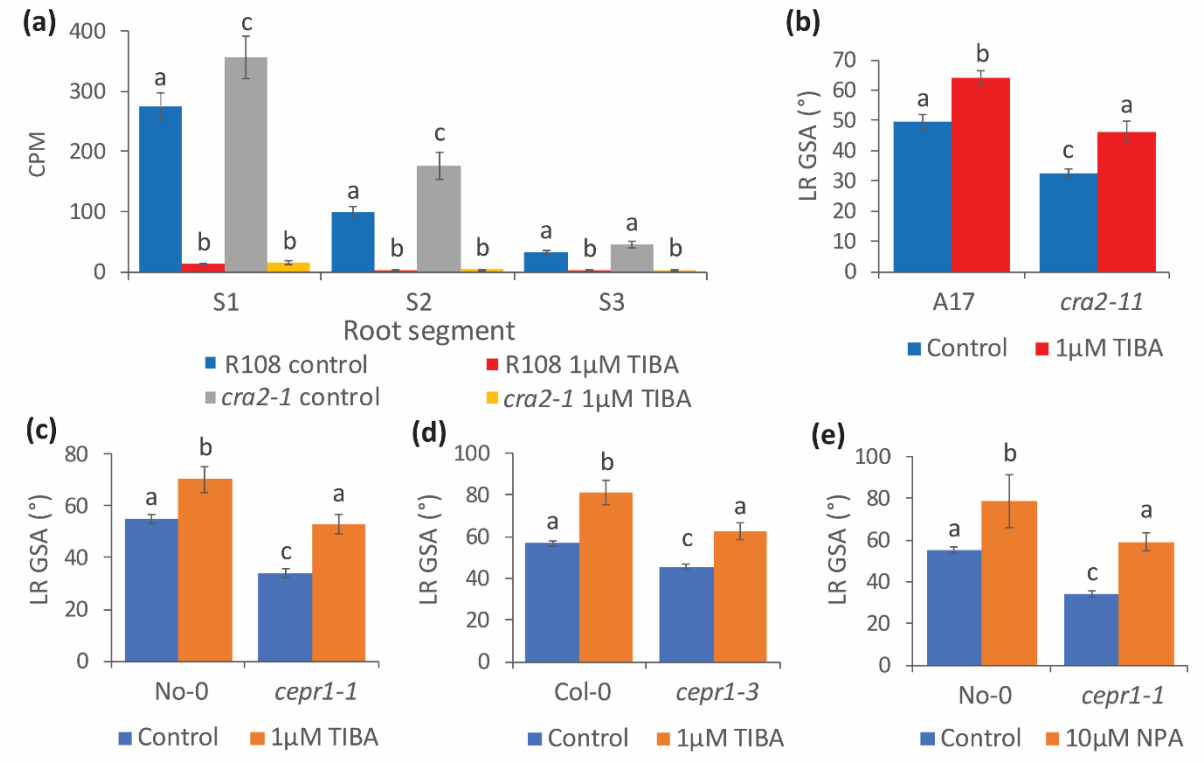

Figure 9. A model for the CEP-CEP receptor control of LR GSA.